



# Prediction of carbon exchanges between China terrestrial ecosystem and atmosphere in 21st century

Ji JinJun<sup>1,2†</sup>, HUANG Mei<sup>1</sup> & LI KeRang<sup>1</sup>

<sup>1</sup> Chinese Ecosystem Research Network, Institute of Geographical Sciences and Natural Resources Research, Chinese Academy of Sciences, Beijing 100101, China;

<sup>2</sup> Institute of Atmospheric Physics, Chinese Academy of Sciences, Beijing 100029, China

**The projected changes in carbon exchange between China terrestrial ecosystem and the atmosphere and vegetation and soil carbon storage during the 21st century were investigated using an atmosphere-vegetation interaction model (AVIM2). The results show that in the coming 100 a, for SRES B2 scenario and constant atmospheric CO<sub>2</sub> concentration, the net primary productivity (NPP) of terrestrial ecosystem in China will be decreased slowly, and vegetation and soil carbon storage as well as net ecosystem productivity (NEP) will also be decreased. The carbon sink for China terrestrial ecosystem in the beginning of the 20th century will become totally a carbon source by the year of 2020, while for B2 scenario and changing atmospheric CO<sub>2</sub> concentration, NPP for China will increase continuously from 2.94 GtC·a<sup>-1</sup> by the end of the 20th century to 3.99 GtC·a<sup>-1</sup> by the end of the 21st century, and vegetation and soil carbon storage will increase to 110.3 GtC. NEP in China will keep rising during the first and middle periods of the 21st century, and reach the peak around 2050s, then will decrease gradually and approach to zero by the end of the 21st century.**

carbon cycle, AVIM2, climate change, B2 scenario, China terrestrial ecosystems

Global climate warming is becoming obvious due to the sharply increasing atmospheric CO<sub>2</sub> which comes from the green house gases emitted by human burning fossil fuel since the industrialization, especially in recent 100 a. According to previous research<sup>[1]</sup>, about half of the CO<sub>2</sub> emissions will remain in the atmosphere for a long time and the balance will be absorbed by ocean and terrestrial ecosystem. The terrestrial ecosystem is one of the largest carbon pools in land surface, and the total carbon accumulated in vegetation biomass and soil organic matter is almost 3 times the atmospheric carbon storage<sup>[2]</sup>. In the coming 100 a, a large amount of human greenhouse gases will continuously be released to the atmosphere, and the atmospheric temperature will continue to rise<sup>[3]</sup>. In this situation, issues like whether the terrestrial ecosystem can keep on absorbing atmospheric CO<sub>2</sub>, and whether it will reach saturation, if yes, when are very important. Since those issues have a bearing on the rate

and magnitude of the future global warming and the future global environment and socio-economic development, long-term direct measurement of CO<sub>2</sub> absorptive rate for a plant is a basic method to estimate the carbon absorptive capacity for a terrestrial ecosystem, but to predict absorption potential for the biosphere in regional and even in global scales in the future, the process-based ecosystem models are absolutely needed.

Many previous researches concerned the future carbon absorption potential for global terrestrial ecosystem. Coupled model simulations indicate that the global terrestrial ecosystem will probably become a carbon source, i.e. the ecosystem will release CO<sub>2</sub> to the atmosphere, at the end of the 21st century<sup>[4,5]</sup>, but with large discrep-

Received September 27, 2007; accepted December 20, 2007

doi: 10.1007/s11430-008-0039-y

†Corresponding author (email: jijj@mail.iap.ac.cn)

Supported by the Basic Research Program of China (Grant No. 2002CB412500) and the National Natural Science Foundation of China (Grant No. 30590384)

ancy in the saturated time and the strength of ecosystem's feedback<sup>[6-9]</sup>. Schaphoff et al.<sup>[10]</sup> reported that the response of ecosystem to climate has large regional difference, e.g., some regions may become increasing carbon sink whereas others may become increasing carbon source under the same future climate change scenario. It is still unclear about the carbon balance of China terrestrial ecosystem in the future 100 a. The atmosphere vegetation interaction model (AVIM2) was used in this study to predict the response of carbon fluxes for China terrestrial ecosystems to the increasing atmospheric CO<sub>2</sub> concentration and the changing climate in the 21st century.

## 1 Model, data and methodology

### 1.1 Description of the model

The model used in this study to simulate carbon exchanges between the ecosystem and the atmosphere is AVIM2, which is the new version of AVIM<sup>[11-14]</sup>. Com-

pared with the original version, a soil carbon and nitrogen dynamics module was added. The model structure is shown in Figure 1, which is divided into 3 parts:

(1) Physical process module (PHY). This module is a typical soil, vegetation and atmosphere biophysical model, which is based on the work of Ji and Hu<sup>[15]</sup> as shown on the left of Figure 1. The main process simulated by this module is the transfer of energy and water among soil, vegetation and the atmosphere. When short wave solar radiation reached the top of canopy, some fractions of it were reflected, the remains were absorbed by the canopy or passed through the canopy and reached to the surface of soil and only a very small part of the radiation was used for photosynthesis. The intensity of reflection, absorption and transmission of the radiant energy is related with the structure of the canopy. The radiation absorbed by canopy is transferred to the atmosphere by the ways of long wave radiation, turbulent heat transfer and evaporation, and only a fraction is used for canopy heating and photosynthesis. The canopy

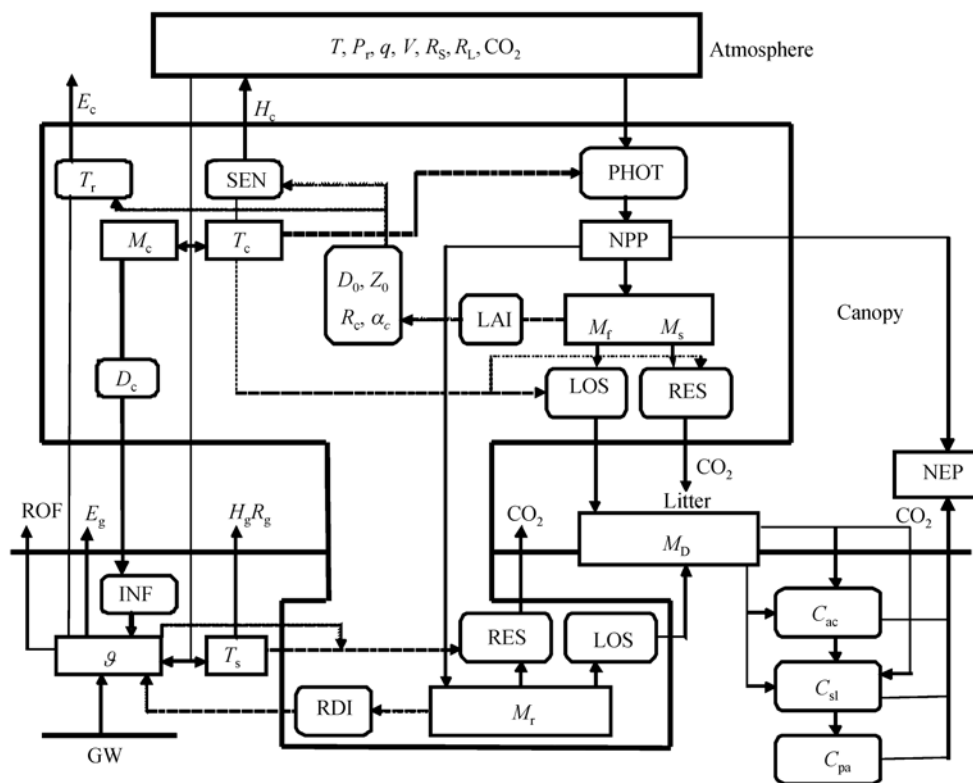


**Figure 1** The structure of AVIM2. The panels from top to bottom are atmosphere, canopy and soil, respectively. Variables  $T$ ,  $q$ ,  $P$ ,  $R_s$ ,  $R_l$  are air temperature, wind velocity, humidity, precipitation, short and long wave radiations, respectively.  $T_c$ ,  $M_c$ ,  $T_s$  and  $\theta$  denote canopy temperature, liquid water content, soil temperature and moisture, respectively.  $M_f$ ,  $M_s$ ,  $M_r$ ,  $M_D$  are biomass of leaf, stem, root and litter dry matter, respectively. Symbols  $C_{ac}$ ,  $C_{sl}$ ,  $C_{pa}$  represent active, slow and passive carbon pools. PHOT, RES, LOS denote photosynthesis, respiration and falling rates. LAI, RDI are leaf area and root density indices.  $R_c$ ,  $Z_0$ ,  $d_0$ ,  $\alpha_c$  are canopy resistance, roughness, zero plant displacement and albedo, respectively. NPP and NEP are net primary productivity and net ecosystem productivity, respectively. The solid arrow in this figure denotes the transfer of water, heat and biomass, and the dash arrow denotes act direction.

temperature is determined by energy budgets. The radiation which passes through the canopy and reaches to the land surface is also reflected and absorbed, and then part of the energy is transferred to the atmosphere by the ways of long wave radiation, turbulent heat transfer and evaporation, and part is input into the soil layer. The thermal condition of soil is determined by the heat conduction equation, and the soil heat conductivity is the function of soil physical properties and soil moisture. The precipitation (or snowfall) arriving at the canopy is accumulated until the amount of water exceeds its capacity and then the superfluous water falls to the ground. The water intercepted by the canopy evaporates to the atmosphere directly. The water reaching ground from the canopy and the atmosphere infiltrates into the soil, and evaporates from ground surface, and if the surface layer of soil is saturated the remains became surface runoff. In the vegetated land surface, the water in soil was absorbed by root and transferred to stoma by stem and leaf, and then transpires to the atmosphere. When there exists a snow cover, the height (or mass) of the snow cover changes with the intensity of the snowfall, snow surface evaporation and snowmelt process<sup>[16]</sup>.

(2) The physiological plant growth module (PLT). This module contains the vegetation eco-physiological process, as shown on the top right of Figure 1, and detailed description of this process can be found in refs. [12,13]. When the atmospheric CO<sub>2</sub> enters into the stoma of leaf, it will carry on the photosynthesis to produce dry matter by the help of enzyme. Eliminating the dry matter lost due to maintenance and growth respiration, the rest is allocated to each organ: leaf, stem and root. The changing rates of biomass for leaf, stem and root are as follows:

$$(1+b)\frac{dM_f}{dt} = \alpha_f(A_c - R_m) - \mu_f M_f, \quad (1a)$$

$$(1+b)\frac{dM_r}{dt} = \alpha_r(A_c - R_m) - \mu_r M_r, \quad (1b)$$

$$(1+b)\frac{dM_s}{dt} = \alpha_s(A_c - R_m) - \mu_s M_s, \quad (1c)$$

where  $M_f$ ,  $M_s$ ,  $M_r$  are biomass of leaf, stem and root, respectively. The subscripts f, s and r denote the variables for leaf, stem and root respectively.  $\alpha_f$ ,  $\alpha_r$  and  $\alpha_s$  are the allocating coefficients of assimilation matter, with  $\alpha_f + \alpha_r + \alpha_s = 1$ .  $\mu_f$ ,  $\mu_r$  and  $\mu_s$  are the litter falling rates. The photosynthesis scheme is based on biochemistry of photosynthesis<sup>[17]</sup>, in which the carboxylation rate is the

function of environment temperature, leaf nitrogen concentration and leaf water potential. The photosynthesis rate, stomata conductance and the CO<sub>2</sub> concentration in stomata are determined by the relationship between the photosynthetic rate and the CO<sub>2</sub> concentration in stomata, the diffusion theory for the CO<sub>2</sub> entering stomata and the experimental correlation between stomata conductance and photosynthesis rate. The maintenance respiration changes with the organic temperature, while the rate of growth respiration is positively correlated with the changing rate of organic biomass. The proportions of assimilation allocated to various organisms are correlated with biological activities<sup>[11]</sup>, and they may change with plant growth. The vegetation phenological phases vary with plant function types and are correlated with temperature. The offset of leaf is decided by its lifespan and phenological phase, while the offset of root and stem occurred randomly with their lifespan<sup>[13,14]</sup>. The difference between the photosynthetic rate and respiration rate is the net primary productivity (NPP):

$$NPP = A_c - R_m - R_g. \quad (2)$$

(3) Soil carbon and nitrogen dynamics module(SOM). This module was newly added to AVIM to constitute a new version AVIM2. The SOM simulates biogeochemical processes such as the transformation and decomposition of soil organic carbon and nitrogen mineralization, as shown in the bottom of Figure 1. It was developed on the basis of soil carbon and nitrogen dynamics modules of CENTURY<sup>[18]</sup> and CEVSA<sup>[19]</sup> with some modifications, and can be coupled directly and timely with modules PHY, PLT. The soil organic matter is stored in eight carbon pools, i.e. structure and metabolic pools for leaf and stem litter, structure and metabolic pools for root litter, soil microbe pool, humus pool, etc. and the change of each carbon pool is determined by the transformation and decomposition of soil organic matter,

$$\frac{dQ_i}{dt} = K_i f(T) f(P) Q_i + d_{ij} Q_j + F, \quad (3)$$

where  $Q_i$  are the carbon density for each pool,  $K_i$  are maximum decomposition rates,  $f(T)$ ,  $f(W)$  are the effects of soil temperature and wetness on decomposition rate,  $d_{ij}$  is the transformational rate between the pools and  $F$  is the input of litter carbon. The partitioning of litter carbon from PLT into structure or metabolic pools depends on the ratio of lignin/N density. The organic carbon is decomposed by microbe and then releases to the atmosphere. The transformation and decomposition

rates of soil organic carbon are related to temperature, wetness, texture and nitrogen concentration in soil layer. Soil temperature and soil wetness come from PHY module. The sum of gaseous carbon releases in soil layer is the heterotrophic respiration,

$$HR = \sum Q_i K_i (1 - \varepsilon), \quad (4)$$

where  $\varepsilon$  is the assimilation efficiency, that is the fraction of decomposed carbon incorporated into microbial tissues. The difference between NPP and HR is NEP.

The temperature and humidity of canopy and soil, which are the outputs of PHY module, together with photosynthetic effective radiation and atmosphere CO<sub>2</sub> concentration, are all act on plant physiological processes, such as photosynthesis, respiration, phenological phases and the transformation and decomposition of organic matter. Meanwhile with plant growing, its morphology and structure, such as leaf area index, and density of root, will also change. The solar radiation reflectivity will vary with the changes of the morphological properties and structure of the plant, and thus cause the changes of land surface kinetic roughness and the canopy stomata resistance, furthermore to influence the water and energy balance of the surface. This is a process containing the interaction and feedback between the surface biophysical and biogeochemical processes. Each process has different time scales: the biophysical process is the fastest one, and its time step is set as half an hour; the photosynthesis and respiration in plant physiological process have diurnal variation as the temperature and humidity change, where time step was set as 1 h; the time steps for the allocation of assimilation, the accumulation of biomass and the decomposition of soil organic matter were set as 1 d.

## 1.2 Data

This study was conducted to predict future carbon exchanges between the terrestrial ecosystem and the atmosphere. The study area covers all China terrene, with the spatial resolution of 50 km × 50 km grid. Soil texture and vegetation type data were obtained by using the ARC-GIS software to resample China soil texture and vegetation type datasets<sup>[20]</sup> which is in 0.1° × 0.1° resolution. The classification of soil texture mainly reflects the proportion of mineral particle's size in soil surface layer and the geographical distribution characteristics of various soil textures. Based on the relative percentages of the content of particle grade, the soil texture was divided

into 12 grades in China, namely, gravel, sand, coal sand, fine sand, silty sand, sandy silt, silt, silty clay, silty loam, loam, loamy clay, and clay<sup>[20]</sup>. To simplify modeling, plant functional type (PFT) is widely proposed as an ecological alternative to traditional ecosystem types. PFTs can be defined as a group of plant species having the same structural and functional characteristics, which represent the predominance of terrestrial ecosystems or the groups of main plant species<sup>[21]</sup>. The PFTs map released by international geosphere–biosphere programme (IGBP) was used in this study, dividing the vegetation in China into 14 PFTs: Evergreen needle leaf forest, evergreen broad leaf forest, deciduous needle leaf forest, deciduous broadleaf forest, mixed forest, closed shrub lands, open shrub lands, woody savannas, grasslands, alpine steppe, croplands, cropland and natural vegetation mosaic, desert steppe and barren or sparse vegetation.

The data used to drive the model in this study were from Xu et al.<sup>[22–24]</sup> who used the regional climate model system developed at Hadley Centre for Climate Prediction and Research, e.g. providing regional climates for impacts studies (PRECIS)<sup>[25]</sup>, to generate the 21st century daily climate change scenarios for China, with a horizontal resolution of 50 km × 50 km. PRECIS is driven with fine resolution (1.875° in longitude and 1.25° in latitude) under the initial and lateral boundary conditions of HadAM3P, which is based on course resolution (3.75° in longitude and 2.5° in latitude) supplied by Hadley Centre coupled ocean-atmosphere model (HadCM3). B2 scenario illustrated in IPCC 2000 Special Report on Emissions Scenarios (SRES)<sup>[26]</sup> was used as the future green house gases emissions assumption. For B2 scenario, population increases at a relatively low rate, with its emphasis on local solution to economic, social and environmental sustainability. Crop lands will increase by about 14% and atmospheric CO<sub>2</sub> will reach to 621 × 10<sup>-6</sup> m<sup>3</sup> · m<sup>-3</sup> in 2100.

The data for China were intercepted from the global 21st century temperature and precipitation datum produced by Hadley Center with the resolution of 3.75° in longitude and 2.5° in latitude. The difference between China regional averaged temperature and precipitation during the 21st century and the averages over the period of 1960–1990 are shown in Figure 2. Figure 2 depicts that both mean temperature and precipitation show increasing tendency in the 21st century. Compared with the year of 2000, the China regional mean temperature



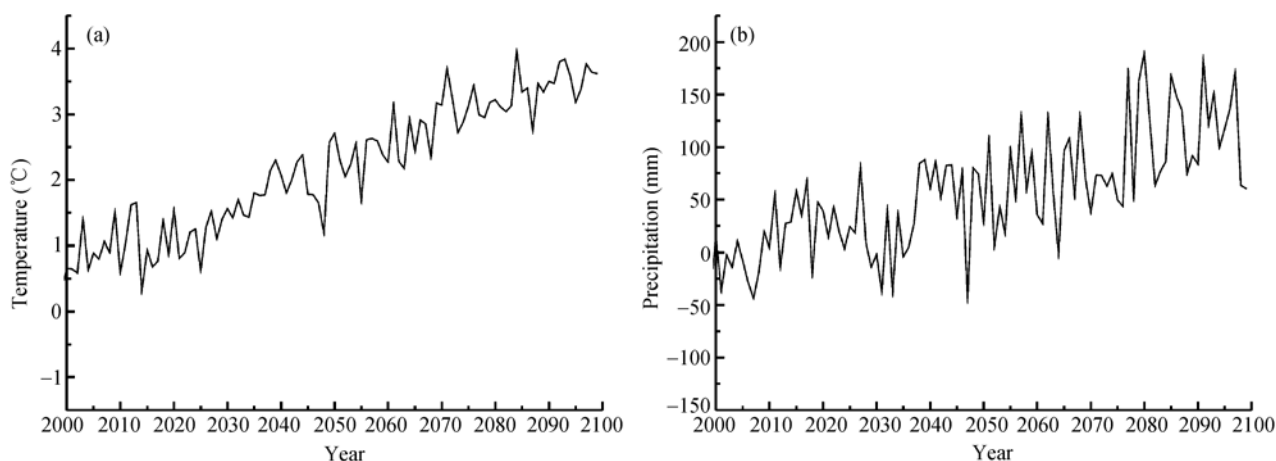


**Figure 2** The temperature and precipitation abnormal in the 21st century for B2 scenario predicted by HadCM3. Data source: The IPCC Data Distribution Centre ([http://cera-www.dkrz.de/IPCC\\_DDC/](http://cera-www.dkrz.de/IPCC_DDC/)).

and precipitation increased by about 3 °C and 100 mm in 2001.

### 1.3 Model experimental design

Two steps were needed to run the model. First, the daily meteorological and atmospheric CO<sub>2</sub> concentration data for 1961 were used to spin up the model to equilibrium status, and then the data for 1961–2100, of which the daily meteorological data for the period of 1961–1990 were taken from measurements, and the meteorological data for 2071–2100 are taken from PRECISE modeling, and those for 1991–2070 were obtained by pattern-scaling method on the basis of global temperature increasing tendency estimated by HadCM3, and the atmospheric CO<sub>2</sub> concentration before 2000 is set to observed values, followed by B2 scenario after 2000, were used to dynamically modeling to get the China terrestrial ecosystem carbon storage and carbon exchanges between the ecosystem and the atmosphere for the period of 1981–2100. To eliminate the influence of initial values (e.g. the influence of equilibrium status assumption) on the outputs, the simulation for the period of 1961 to 1980 was excluded. Two schemes were conducted in predictions in the 21st century: One was that the atmospheric CO<sub>2</sub> concentration would remain the value of 2000 and climate would change under B2 scenario (constant CO<sub>2</sub> B2, hereafter), the other was that both the CO<sub>2</sub> concentration, and climate would change under the B2 scenario (changing CO<sub>2</sub> B2, hereafter). The comparison of the two schemes was made to estimate the fertilization effects of atmospheric CO<sub>2</sub> concentration on ecosystem.

## 2 The spatial distribution of carbon exchanges between China terrestrial ecosystem and the atmosphere

AVIM has been used to simulate the surface physical and the ecosystem carbon fluxes on global and regional scales, and has been previously validated and tested many times. Li et al.<sup>[27]</sup> and Dan et al.<sup>[28]</sup> used AVIM to simulate the global NPP with the climatic mean data and compared the results with measurements, and Huang et al.<sup>[29]</sup> used AVIM2 to simulate and analyze the vegetation root and shoot biomass. For China subtropical red soil plants (Qianyanzhou), Huang et al.<sup>[14]</sup> compared and analyzed the simulated GPP, NPP and NEP with the data deduced from the eddy covariance CO<sub>2</sub> flux measurements and got good results. AVIM2 ever took part in the model comparison project of PILPS-C, and compared the modeled carbon fluxes with the filed measurements in Loobos site, Holland (<http://www.pilpsc1.cnrs-gif.fr/>).

Although some uncertainties occur in the projection of the carbon fluxes of ecosystems, the modeling confidence still can be estimated by comparing the ecosystem carbon exchanges with previous researches and statistical data.

### 2.1 Comparisons of estimated total carbon exchanges between China ecosystems and the atmosphere with other researches

The following is the comparison of the simulated total soil and vegetation carbon storage, and the total carbon exchanges between China ecosystems and the atmosphere with other researches, in which some of them were obtained from field measurements and the others

are deduced from remote sensing data. Table 1 shows the value for AVIM2 simulation averaged over 1981–2000. In terms of the total soil carbon in 1 m soil layer in China, AVIM2 estimation is 82.77 GtC, being close to the reports of Li et al. (82.65 GtC)<sup>[30]</sup>, and Li et al. (83.8 GtC)<sup>[31]</sup> as well as Xie et al. (84.4 GtC)<sup>[32]</sup>, and lower than the results of Wang et al.<sup>[33]</sup> and Yu et al.<sup>[34]</sup>, which are 92.4 and 89.14 GtC, and higher than the estimation of Wu et al.<sup>[35]</sup>(70.2 GtC). All estimation of soil carbon storage used for comparison was derived from the China-wide soil inventory, except for the results of Li et al.<sup>[30]</sup>. Since the gaps exist in studying methods, spatial resolutions and the research periods, the difference in estimation is understandable. Comparisons show that AVIM2 estimation of the soil carbon storage during the period of 1981–2000 is reasonable.

AVIM2 estimation of the total NPP in China is 2.94 GtC·a<sup>-1</sup>, which is close to the CEVSA model simulation value of 3.09 GtC·a<sup>-1</sup> reported by Tao et al.<sup>[36]</sup>, and higher than the reports of Sun et al.<sup>[37]</sup> (2.645 GtC·a<sup>-1</sup>) and Piao et al.<sup>[38]</sup>(1.95 GtC·a<sup>-1</sup>), and lower than the value of 3.653 GtC·a<sup>-1</sup> estimated by Xiao<sup>[39]</sup>. The estimation of Sun et al.<sup>[37]</sup>, Piao et al.<sup>[38]</sup> and Xiao<sup>[39]</sup> was independently derived from the remote sensing data.

In terms of total vegetation carbon in China, AVIM2 estimation is 13.74 GtC which is slightly less than the value of 14.04 GtC reported by Huang et al.<sup>[29]</sup> who used the same model with a different spatial resolution of 0.1°×0.1° grids. The estimation in this study is also close to the CEVSA model simulation value of 13.33 GtC<sup>[30]</sup>.

AVIM2 estimation of total soil respiration and NEP is 2.84 and 0.10 GtC·a<sup>-1</sup>. The estimated total respiration is

slightly lower than the value of 3.02 GtC·a<sup>-1</sup> reported by Cao et al.<sup>[40]</sup> and the estimated NEP is a little higher than their estimation of 0.07 GtC·a<sup>-1</sup>.

## 2.2 The spatial distribution of NPP in China averaged over 1981–2000

Vegetation net primary productivity (NPP) is the residue of vegetation gross primary productivity minus gross respiration, e.g., the carbon exchange rate between the vegetation and the atmosphere. NPP geographical pattern in China, which is consistent with the precipitation, shows the highest value in southeast and the lowest in northwest. Figure 3(a) shows the model-estimated NPP distribution in China averaged over 1981–2000. The highest NPP, located in Yunnan, Guizhou, Sichuan and southeastern coast areas mainly covered by broadleaf forests, is between 800 and 1000 gC·m<sup>-2</sup>·a<sup>-1</sup>. The NPP between 600 and 800 gC·m<sup>-2</sup>·a<sup>-1</sup> distributes in the east of northeast China, western Sichuan, and the south and southeast of Tibet forest areas. In the eastern crop land and crop and forest mixed areas, the NPP is between 400 and 600 gC·m<sup>-2</sup>·a<sup>-1</sup>. From western Inner Mongolia to the eastern part of Qinghai-Tibet Plateau along the western semi-arid grassland, NPP is about 200–300 gC·m<sup>-2</sup>·a<sup>-1</sup>. The vegetation NPP in arid and desert area in northwestern China and western Tibetan Plateau is lower than 100 gC·m<sup>-2</sup>·a<sup>-1</sup>. In general, this geographical distribution is consistent with the other researches<sup>[28,36,41]</sup>.

## 2.3 The spatial distribution of NEP in China averaged over 1981–2000

Net ecosystem productivity (NEP) is the residue of NPP minus soil heterotrophic respiration, e.g., the carbon

**Table 1** Comparison of AVIM2 estimation of total carbon fluxes and storages in China terrestrial ecosystems averaged over 1981–2000 with other researches<sup>a)</sup>.

$C_s$ (GtC)	AVIM2	Wang et al. <sup>[33]</sup>	Wu et al. <sup>[35]</sup>	Li et al. <sup>[30]</sup>	Xie et al. <sup>[32]</sup>	Li et al. <sup>[31]</sup>	Yu et al. <sup>[34]</sup>
	82.77	92.4	70.3	82.65	84.4	83.8	89.14
NPP (GtC·a <sup>-1</sup> )	AVIM2	Xiao <sup>[39]</sup>	Sun et al. <sup>[37]</sup>	Piao et al. <sup>[38]</sup>	Tao et al. <sup>[36]</sup>		
	2.94	3.653	2.645	1.95	3.09		
$C_v$ (GtC)	AVIM2	Li et al. <sup>[30]</sup>	Huang et al. <sup>[29]</sup>				
	13.74	13.33	14.04				
$R_s$ (GtC·a <sup>-1</sup> )	AVIM2	Cao et al. <sup>[40]</sup>					
	2.84	3.02					
NEP (GtC·a <sup>-1</sup> )	AVIM2	Cao et al. <sup>[40]</sup>					
	0.10	0.07					

a)  $C_s$ : Total soil carbon,  $C_v$ : Total vegetation carbon,  $R_s$ : Total soil respiration.

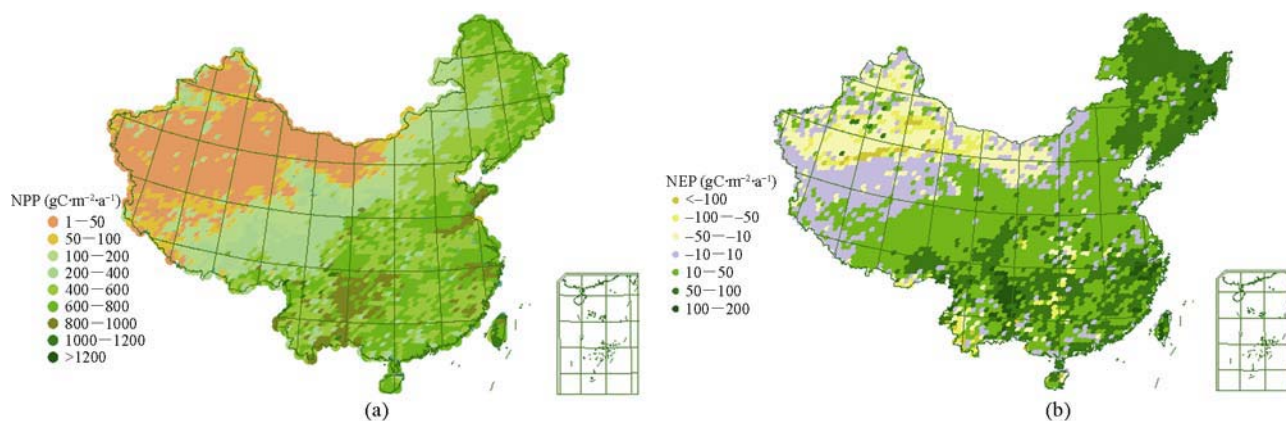


Figure 3 The spatial distribution of simulated NPP ( $\text{gC} \cdot \text{m}^{-2} \cdot \text{a}^{-1}$ ) (a) and NEP ( $\text{gC} \cdot \text{m}^{-2} \cdot \text{a}^{-1}$ ) (b) in China averaged over 1981–2000.

exchange rate between the ecosystem and the atmosphere. Except for northwestern arid area and a few individual areas in south where there are weak carbon sources (NEP is negative) (Figure 3(b)), and most of the areas in China are carbon sinks (NEP is positive). The strongest carbon sinks of about  $50\text{--}100 \text{ gC} \cdot \text{m}^{-2} \cdot \text{a}^{-1}$ , occur in the northeastern, southeastern and southwestern forests, in which a few forest NEP is more than  $100 \text{ gC} \cdot \text{m}^{-2} \cdot \text{a}^{-1}$ , followed by carbon sinks for the eastern crops and the vast grasslands, which are between  $10\text{--}50 \text{ gC} \cdot \text{m}^{-2} \cdot \text{a}^{-1}$ . The semi-desert area is a weak carbon sink, and NEP is all below  $10 \text{ gC} \cdot \text{m}^{-2} \cdot \text{a}^{-1}$ . In general, areas covered by vegetation are more or less carbon sinks, reflecting the atmospheric  $\text{CO}_2$  fertilization effects. The carbon sink is strong in the northeast and the southern area of the Yangtze River basin with higher precipitation.

### 3 China terrestrial ecosystems' carbon storage and carbon exchanges with the atmosphere in the 21st century

As described in subsection 1.3, the future atmospheric  $\text{CO}_2$  concentration was taken as constant or variable to drive the model to get the terrestrial ecosystem carbon storage and carbon fluxes in the future. The following are the analysis of the temporal and spatial distribution of the simulations.

#### 3.1 The temporal changes of China terrestrial ecosystems' carbon storage and exchanges with atmosphere in the 21st century

(1) The change of total NPP in China. Figure 4(a) displays the changes of 10-year moving averaged total

NPP of China during 1981–2100. The averaged total NPP over 1981–2000 is  $2.94 \text{ GtC} \cdot \text{a}^{-1}$ . For constant  $\text{CO}_2$  B2, the simulated total NPP will be decreased and fluctuated from the year of 2000, and it will decrease to about  $2.49 \text{ GtC} \cdot \text{a}^{-1}$  in the year of 2100, with a net decrease of  $0.45 \text{ GtC} \cdot \text{a}^{-1}$ . For changing  $\text{CO}_2$  B2, the simulated total NPP will increase gradually. It will reach  $3.99 \text{ GtC} \cdot \text{a}^{-1}$  in 2100, with the increase of 35.7%. The vegetation totally absorbs extra  $1.5 \text{ GtC} \cdot \text{a}^{-1}$  due to the fertilization effects of increasing  $\text{CO}_2$ .

The estimated decrease in total NPP for constant  $\text{CO}_2$  B2 is mainly related to the temperature increasing projection. As predicted by regional climate model<sup>[21]</sup>, the summer temperature during 2071–2100 will increase by above  $4.0^\circ\text{C}$  on the north of  $40^\circ\text{N}$  latitude in China, and on the south of  $40^\circ\text{N}$  latitude, the summer air temperature will increase by  $2\text{--}4^\circ\text{C}$ , while the winter air temperature will increase by more than  $3.5^\circ\text{C}$ . Meanwhile the summer precipitation in the north of Yangtze River will decrease by  $1 \text{ mm} \cdot \text{d}^{-1}$ , and that in the southeastern China will increase by about  $1.5 \text{ mm} \cdot \text{d}^{-1}$  in average. The evapotranspiration in northern China will be increased under this climate change scenario. That combining with the decrease in precipitation will make drought intensified, and limit the photosynthesis. Meanwhile, the increase in temperature makes respiration and consumption increase, resulting in NPP decline. In southern China, air temperature is not the major factor to constrain NPP, but it also causes increasing respiration, so NPP decreases. The photosynthesis will be directly enhanced by increasing  $\text{CO}_2$ . The predicted atmosphere  $\text{CO}_2$  concentration will be  $621 \times 10^{-6} \text{ m}^3 \cdot \text{m}^{-3}$  ppmv at the end of the 21st century, this value is still

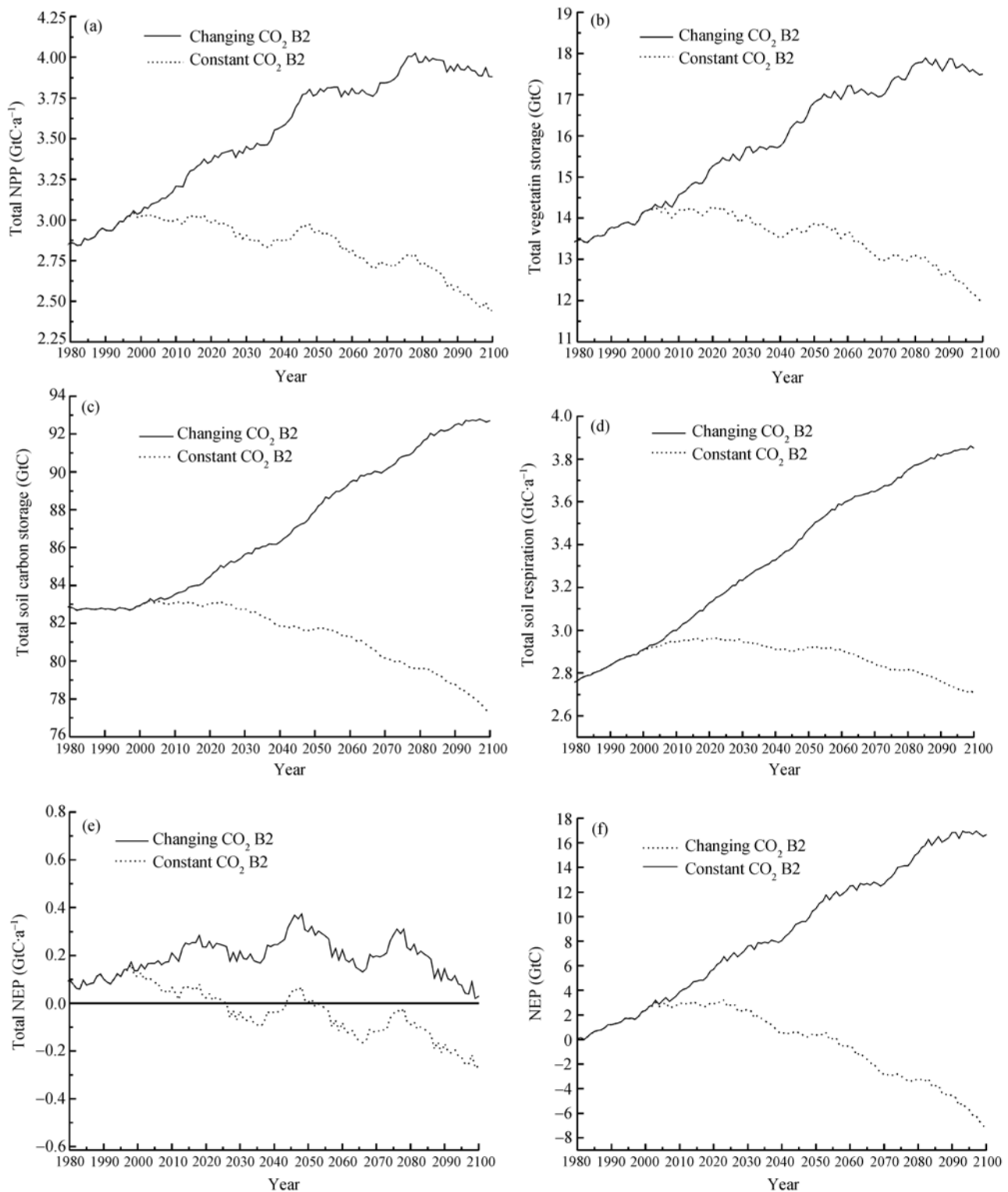


**Figure 4** Simulated changes of NPP (a), vegetation carbon (b), soil carbon (c), soil respiration (d), NEP (e) and accumulated NEP (f) in China during 1981–2100 for the constant CO<sub>2</sub> and changing CO<sub>2</sub> assumptions.

less than the saturated concentration for photosynthesis by current understanding<sup>[42]</sup>. Therefore, increasing photosynthesis makes NPP increase, and more carbon in the

atmosphere will be absorbed.

The projected future NPP tendencies in China are consistent with global NPP predictions made by Cramer



et al.<sup>[6]</sup>, Schaphoff et al.<sup>[10]</sup> and Ito<sup>[43]</sup>. Cramer et al.<sup>[6]</sup> compared 6 models' simulation of global carbon exchanges between ecosystems and atmosphere under future changing CO<sub>2</sub> and climate scenarios. For constant CO<sub>2</sub> and climate scenarios, the predicted global NPP showed decreasing tendency in all 6 models' simulations, whereas for the changing CO<sub>2</sub> and the same climate scenarios, all simulations showed increasing tendency, and the average NPP increase will be 33% in 2100, which is slightly lower than this study (35.7%).

(2) The changes of soil and vegetation carbon storage. Figure 4(b) and c is the variations for total vegetation and soil carbon in China for the two B2 assumptions, in which changes in total vegetation and soil carbon storage show the similar trends to those of NPP. For the constant CO<sub>2</sub> B2, total vegetation carbon will decrease from 13.91 GtC at the late 20th century to 12.29 GtC at the end of the 21st century with a net decrease of 1.62 GtC, while the total soil carbon will decrease from 82.78 to 77.98 GtC, with a net decrease of 4.8 GtC. Because of increasing CO<sub>2</sub> fertilization effect, the total vegetation carbon will increase to 17.62 GtC at the end of the 21st century with a net increase of 3.71 GtC, meanwhile soil carbon will increase to 92.67 GtC, with a net increase of 9.89 GtC.

When the fertilization effects of increasing atmospheric CO<sub>2</sub> are not considered, total vegetation and soil carbon storage for China terrestrial ecosystem will be 90.27 GtC at the end of the 21st century, which is 6.42 GtC less than the value at the end of the 20th century. Whereas, when the fertilization effects are considered, the total vegetation and soil carbon will increase from 96.69 to 110.30 GtC, indicating that for constant B2 with the main characteristic of increasing temperature, the carbon storage in terrestrial ecosystems will continue to be decrease. The fertilization effects caused by increasing CO<sub>2</sub> concentration will significantly influence vegetation by no later than the end of the 21st century. That is to say, the atmospheric CO<sub>2</sub> emitted by human activities will continuously be absorbed and stored in terrestrial ecosystems. This result is consistent with the tendency of carbon storage in global terrestrial ecosystems in the next 100 years<sup>[6,19]</sup>. Cramer et al.<sup>[6]</sup> estimated that from the end of the 20th century to the end of the 21st century, the global vegetation carbon will increase from 680 to 1050 GtC, that is, increasing by 54.4%. Cao et al.<sup>[19]</sup> predicted that in the 21st century, the doubling atmospheric CO<sub>2</sub> concentration will in-

crease vegetation carbon by about 20.8%.

(3) The change of soil heterotrophic respiration. Soil respiration is very sensitive to temperature change. The increasing trend of soil respiration is consistent with the increase of temperature, although a lot of uncertainties exist<sup>[44-47]</sup>. Figure 4(d) shows predicted total soil respiration in the 21st century. For constant CO<sub>2</sub> B2, total soil respiration will decrease from 2.88 to 2.72 GtC·a<sup>-1</sup> in the coming 100 a. The decreased total soil respiration is attributed to the decrease of total carbon storage, whose effects on soil respiration are opposite to those of temperature increase, and the latter is slightly bigger than the former. For changing CO<sub>2</sub> B2, the two effects mentioned above are consistent with each other, so the soil respiration rises rapidly, its intensity will reach 3.84 GtC·a<sup>-1</sup> by the year of 2100, and the increase rate will be 33.6%.

(4) The changes of NEP. NEP is named ecosystem carbon sink (positive value) or carbon source (negative value). It is a key characteristic to measure ecosystem carbon uptake or release. Theoretically, when an ecosystem matures, e.g. climax, it is in equilibrium with the climate and soil environment, so the carbon uptake and release are balanced, and NEP approximates to zero. But if the environmental conditions, such as climate, changed, the ecosystem carbon budgets will not be balanced. We have assumed that China ecosystem approximated to equilibrium status in 1961 in subsection 1.3, and the future ecosystem carbon budget will be based on this reference year. The model estimation indicated that China terrestrial ecosystem is a weak sink at the end of the 20th century, with the total NEP of 0.10 GtC·a<sup>-1</sup>. For the constant CO<sub>2</sub> B2, NEP will become negative at 2020, i.e. the ecosystem will be changed from carbon sink to carbon source at that time, and the carbon source will continue to be intensified after 2020, which will reach -0.253 GtC·a<sup>-1</sup> (Figure 4(e)) at the end of the 21st century. In the 2030s, the total carbon sink accumulated from 2000 in China terrestrial ecosystems will approach to zero, and the accumulated carbon release will reach to about 7 GtC by the year of 2100 (Figure 4(f)). For constant CO<sub>2</sub> B2, the NPP, vegetation and soil carbon storage of China ecosystems will decrease due to increase of temperature, therefore the ecosystem net uptake of carbon will decrease, the carbon sink will change to source gradually, and China ecosystems will release CO<sub>2</sub> to the atmosphere.

The predicted carbon budgets of terrestrial ecosystem for changing CO<sub>2</sub> B2 display a different characteristic from that for constant CO<sub>2</sub> B2. For changing CO<sub>2</sub> B2, NEP will continuously increase from the end of the 20th century, and will reach a maximum around 2050, and then will decrease to approach zero at the end of the 21st century (Figure 4(e)). This result is consistent with the global NEP tendency estimations<sup>[4,6,43,47]</sup>. Figure 4(f) shows that the total uptake of China terrestrial ecosystems is about 16.5 GtC during 1981–2100 for changing atmospheric CO<sub>2</sub>, B2. Eliminating 2 GtC absorbed in the 20th century, the net uptake in the 21st century is about 14.5 GtC, which is equal to about  $7 \times 10^{-6} \text{ m}^3 \cdot \text{m}^{-3}$  atmospheric CO<sub>2</sub>, and is 0.06% of the increase of atmospheric CO<sub>2</sub> under the B2 scenario in the 21st century.

### 3.2 The spatial distribution of the carbon exchanges between China terrestrial ecosystems and the atmosphere in the 21st century

The carbon budgets for China terrestrial ecosystems in the coming 100 a were analyzed before. Since the responses of various ecosystems to climate and atmospheric CO<sub>2</sub> change are different, the spatial distribution of carbon fluxes will change with time. The time sectors of 2001–2020, 2041–2060 and 2081–2100 are assumed to represent the early, middle and late periods of the 21st century, respectively. The NPP and NEP for B2 changing CO<sub>2</sub> and climate scenario were averaged over the three periods. The difference between the averaged NPP and NEP for each period and those averaged over 1981–2001 were used to discuss the spatial and temporal variations of the carbon fluxes for China terrestrial ecosystems.

(1) The variations of NPP spatial distribution. Figures 5(a), (c) and (e) shows the spatial variation of NPP abnormal in the early, middle and late periods in the 21st century, which is the residue of the averaged NPP over the early, middle and late periods minus the NPP averaged over 1981–2000. Compared with NPP in the end of the 20th century, NPP in the early period of the 21st century will increase in most areas in China, especially in the northern China, Yangtze River basin and southwestern and southern China mainly covered by crops or forest and crops mixture, and the increased NPP will be  $50\text{--}200 \text{ gC} \cdot \text{m}^{-2} \cdot \text{a}^{-1}$ . The decreased NPP can be found in a few arid areas in the north of Xinjiang. In the middle of the 21st century, the NPP increasing tendency is

more obvious, with most NPP intensified areas distributing in the southwestern China. The decreased areas of NPP in Xinjiang in the early period of the 21st century will be enlarged during the middle period of the 21st century. In the late period of the 21st century, the spatial distribution of NPP tendency does not change much compared with the former periods but the intensity increased. Most enhanced NPP areas are distributed in the east of Tibetan Plateau and the north of northeastern China. The decreasing NPP in Xinjiang arid area is still unchanged. The spatial and temporal changes of NPP are closely correlated with the increase of temperature and the changing precipitation. Precipitation will increase in most areas in China by the year of 2080 except for the south of northeastern China, the middle and upper reaches of the Yangtze River and south coast zones, where there exist decrease in precipitation and small increased NPP. In the southeastern coast areas with increasing precipitation, since the increase in precipitation is accompanied by increasing clouds cover and decreasing sunlight and radiation, the increased NPP is small. The decreased NPP in northwest arid area is correlated with the rapidly increasing of temperature and the decreasing of precipitation. The constraint of temperature on vegetation NPP in the Tibetan Plateau will be relieved more or less, so NPP will increase sharply.

Various ecosystems have different responses to the variation of atmospheric CO<sub>2</sub>, temperature and precipitation. Table 2 shows the difference between NPP in the early, middle and late periods of the 21st century and NPP in the late period of the 20th century for forest, shrubland, grassland, crops and desert. Except for decreasing NPP in desert ecosystem, NPP for other ecosystems increases. The NPP increasing rates of shrubland, grassland and crops will reach the maximum at the late period of the 21st century, while the rate of forest will reach its maximum at the middle period of the 21st century. The NPP increasing rates of grassland and crops are much greater than those of other ecosystems, which will increase by 152 and 140  $\text{gC} \cdot \text{m}^{-2} \cdot \text{a}^{-1}$  at the end of the 21st century compared with those at the end of the 20th century.

(2) The variations of NEP spatial distribution. As discussed in the last section, for the changing CO<sub>2</sub> B2, China's total NEP will reach the maximum in the mid-21st century and then continuously decline, and will approach to zero by the end of the 21st century. The

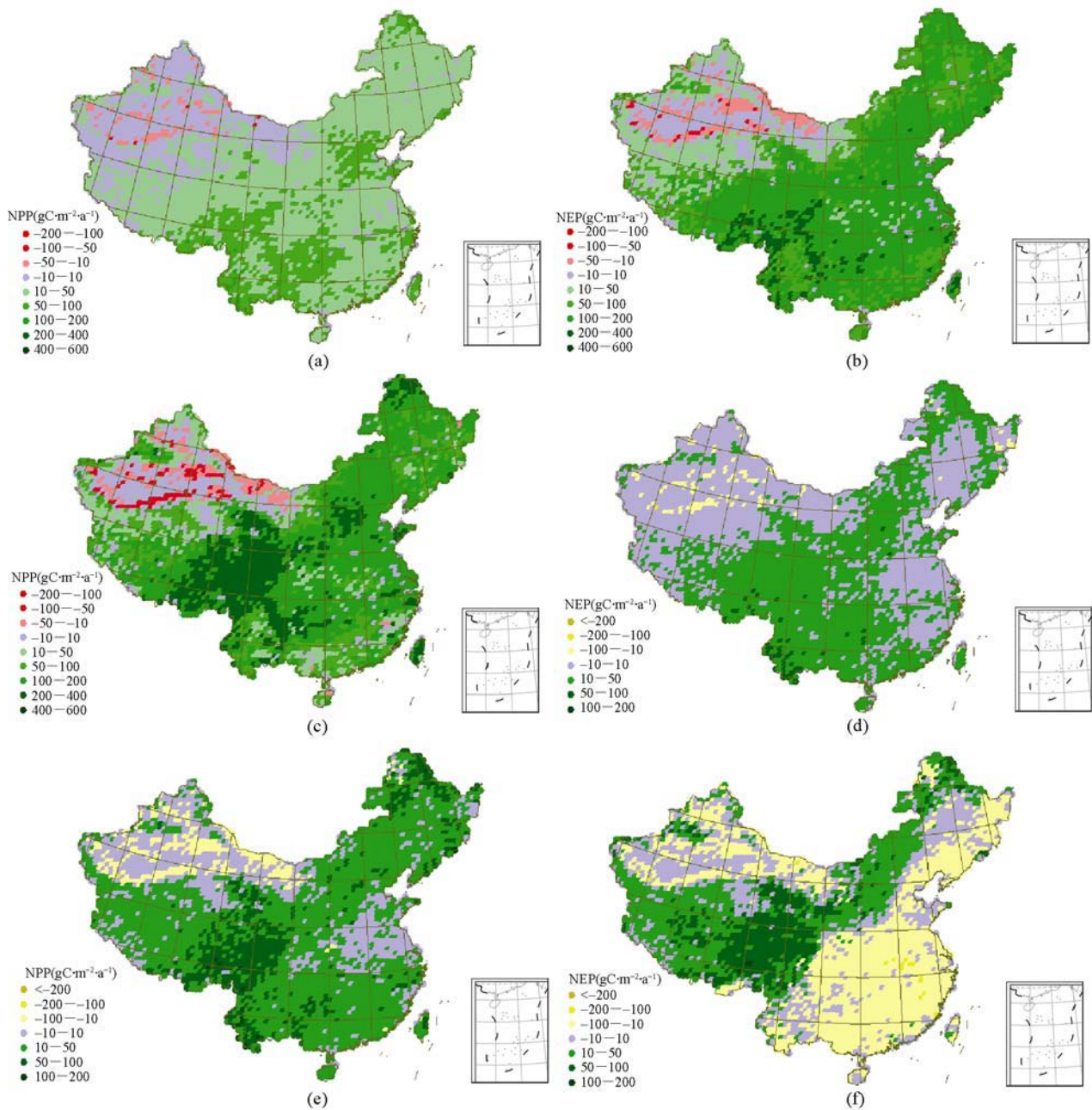


**Figure 5** The differences between NPP ( $\text{gC} \cdot \text{m}^{-2} \cdot \text{a}^{-1}$ ) and NEP ( $\text{gC} \cdot \text{m}^{-2} \cdot \text{a}^{-1}$ ) for B2 scenario averaged over the future periods and the corresponding values averaged over 1981–2000. (a) NPP abnormal for 2001–2020; (b) NEP abnormal for 2001–2020; (c) NPP abnormal for 2041–2060; (d) NEP abnormal for 2041–2060; (e) NPP abnormal for 2081–2100; (f) NEP abnormal for 2081–2100.

**Table 2** The differences between NPP and NEP in the early, middle and late periods of the 21st century and in the period of 1981–2000 for various ecosystems ( $\text{gC} \cdot \text{m}^{-2} \cdot \text{a}^{-1}$ )

Period	Forest		Shrubland		Grassland		Cropland		Desert	
	NPP	NEP	NPP	NEP	NPP	NEP	NPP	NEP	NPP	NEP
2001–2020	48.5	23.3	19.00	12.8	30.0	8.0	40.0	5.2	-31.5	-34.9
2041–2060	126.2	41.1	54.1	26.9	112.3	28.2	124.8	10.7	-26.9	-38.8
2081–2100	104.1	-22.0	61.9	18.4	152.2	15.9	140.0	-19.9	-25.6	-43.7



changes of NEP are different in ecosystems. Figures 5 (b), (d) and (f) shows the spatial distribution of difference of the NEP in the early, middle and late periods of the 21st century and in the end of the 20th century. NEP will firstly decrease in the east of northeastern China and the northwest arid carbon source area. The carbon sinks in southwestern and northern China and the east of Tibetan Plateau will increase in the early 21st century. In the middle 21st century, NEP in Xinjiang will further decrease and the decreasing area is much larger than that in the early 21st century, whereas NEP in the other areas will continuously increase. In the end of the 21st century, NEP will decrease in the whole eastern, southern and northwestern China, while increasing in the semi-arid zone and Tibetan Plateau. The sharp drops of NEP in northern China are correlated with the rapid increasing in soil respiration which is caused by the intense temperature increasing.

The differences between NEP in the early, middle and late periods of the 21st century and those in the late period of the 20th century for various ecosystems are displayed in Table 2. In the early and middle periods of the 21st century, NEP for forests, shrublands and crops will all be increased, especially in the middle of the 21st century. However, NEP for forests and crops in the late period of the 21st century are all lower than that in the end of the 20th century, and that for shrublands and grasslands is lower than that in the middle 21st century. NEP for desert ecosystem in each period of the 21st century is lower than that in the end of the 20th century.

#### 4 Discussions and conclusions

The soil and vegetation carbon storage and the spatial and temporal variation of NPP and NEP for China terrestrial ecosystems in the coming 100 a were simulated by AVIM2 for carbon emission scenario B2 with regional sustainable development. The preliminary conclusions are given in the following paragraph.

For constant CO<sub>2</sub> B2, NPP for China terrestrial ecosystems will gradually decrease in the future because the effect of warming on ecosystem respiration is much greater than the effect on photosynthesis rate. Meanwhile, vegetation and soil carbon storage will decrease. The total soil respiration will have little changes in the future because the decreased soil carbon storage offsets some warming effects, therefore, NEP will decrease as NPP decreases. The carbon sink in the early 21st century

in China will be changed to a source after about 20 a.

For changing CO<sub>2</sub> B2, the projected carbon storage and fluxes in China ecosystems display more different tendencies in the coming 100 a. The effects of increasing CO<sub>2</sub> enhance directly photosynthesis rate and accelerate the accumulation of dry matter, so total NPP continuously increases from 2.94 to 3.99 GtC·a<sup>-1</sup>, in spite of the plant respiration increased with the increasing temperature. Part of the carbon added into the ecosystem will be stored in plants and part in soils. The vegetation and soil carbon storage will increase from 13.91 to 17.62 and 82.78 to 92.67 GtC, respectively. At the end of the 21st century, the total vegetation and soil carbon storage will increase to 110.3 GtC. Meanwhile, soil respiration will increase due to the increased soil carbon pool. Therefore, after an increasing period, NEP will reach the maximum value and then decrease. At the end of the 21st century, NEP will approach to 0 and the vegetation and soil carbon pools will rise gradually.

The responses for various ecosystems to changing CO<sub>2</sub> and climate for B2 will be different in the coming 100 a. The responses of forests and crops will be much stronger than those of grasslands and shrublands. More changes will be found in the middle and late periods of the 21st century. In summary, the carbon sinks in eastern and southern China and northwestern arid areas will gradually change to carbon sources in the late period of the 21st century, while the weak carbon sink will exist in the semi-arid area from the western part of northeast China to the eastern part of the Qinghai-Tibet Plateau.

The above results are obtained under the B2 scenario, in which the CO<sub>2</sub> emission is less than the average level compared with other scenarios, and the temperature increasing in global and China is relatively low, e.g. the averaged increasing temperature over China will be about 3°C at the end of the 21st century. For higher carbon emission scenario, such as A2, the atmospheric CO<sub>2</sub> concentration will increase to about  $720 \times 10^{-6} \text{ m}^3 \cdot \text{m}^{-3}$  and the averaged temperature increasing over China will be about 5°C at the end of the 21st century. Under such situation, the changes for carbon storage and carbon fluxes in China ecosystems will be more intense, the date when the carbon sink turns into source will be earlier. Therefore, this paper presents a prediction of possible change for carbon storage and fluxes under the global and regional sustainable development.



In this study, there exist uncertainties in the unchanged surface coverage in modeling (Global land cover change was included in B2 scenario, and it has a certain proportion to the growth of population), which will, to some extent, underestimate the carbon emissions from land cover changes. On the other hand, since China has been implementing a large-scale afforestation in recent decades, plantations in many areas are still young, whose capacity for assimilate carbon is much greater than the assumed mature forest stands in modeling. Therefore, carbon absorbed by forests was underestimated. Furthermore, in the coming century, the distinct increasing temperature will be the main characteristic of climate change, and there will be subsequent changes in the structure, function, and spatial distribution of ecosystems, combining with a slow adaptation and evaluation process, which will change the carbon storage and

fluxes in ecosystems. The above processes were not included in the simulation. In addition, though the effects of soil nitrogen, soil texture and soil temperature and humidity were considered in the soil carbon and nitrogen dynamics process in AVIM2, there still have been some uncertainties in the parameterization of these processes due to their complication so as to influence the intensity of ecosystem carbon fluxes.

In conclusion, the projected temporal and spatial changes for NPP, vegetation and soil carbon storage and NEP in China's ecosystems in the coming 100 a presented in this paper are a preliminary result, many efforts have to be made to reduce the uncertainties in modeling and to modify the estimation.

*The climate data under SRES B2 scenario projected by PRECIS were from Pro. XU Yinlong who is currently working at Institute of Environment and Sustainable Development in Agriculture, Chinese Academy of Agricultural Sciences.*

- 1 Houghton J T, Meira F, Callander L G, et al. Climate change 1995. The Science of Climate Change. Cambridge: Cambridge University Press, 1995. 65—131
- 2 Houghton R A. The contemporary carbon cycle. In: Schlesinger W H, ed. Biogeochemistry. Oxford: Elsevier-Pergamon, 2003. 473—513
- 3 IPCC. Climate change 2001: The scientific basis. The Carbon Cycle and Atmospheric Carbon Dioxide. Cambridge: Cambridge University Press, 2001. 184—237
- 4 Cox P M, Betts R A, Jones C D, et al. Acceleration of global warming due to carbon-cycle feedbacks in a coupled climate model. *Nature*, 2000, 408: 184—187
- 5 Joos F, Prentice I C, Sitch S, et al. Global warming feedbacks on terrestrial carbon uptake under the Intergovernmental Panel on Climate Change (IPCC) emission scenarios. *Glob Biogeochem Cycle*, 2001, 15: 891—907
- 6 Cramer W, Bondeau A, Woodward F I, et al. Global response of terrestrial ecosystem structure and function to CO<sub>2</sub> and climate change: results from six dynamic global vegetation models. *Glob Change Biol*, 2001, 8: 357—373
- 7 Jones C D, Cox P M, Essery R L H, et al. Strong carbon cycle feedbacks in a climate model with interactive CO<sub>2</sub> and sulphate aerosols. *Geophys Res Lett*, 2003, 30(9): 1479—1483
- 8 Friedlingstein P, Dufresne J L, Cox P M, et al. How positive is the feedback between climate change and the carbon cycle? *Tellus Ser B-Chem Phys Meteorol*, 2003, 55: 692—700
- 9 Berthelot M, Friedlingstein P, Clais P, et al. How uncertainties in future climate change predictions translate into future terrestrial carbon fluxes. *Glob Change Biol*, 2005, 11: 959—970
- 10 Schaphoff S, Lucht W, Gerten D, et al. Terrestrial biosphere carbon storage under alternative climate projections. *Clim Change*, 2006, 74: 97—122
- 11 Ji J J. A climate-vegetation interaction model: Simulating physical and biological processes at the surface. *J Biogeogr*, 1995, 22: 2063—2069
- 12 Ji J J, Huang M, Liu Q. Modeling studies of response mechanism of steppe productivity to climate change in middle latitude semiarid regions in China. *Acta Meteorol Sin (in Chinese)*, 2005, 63(3): 257—266
- 13 Lu J, Ji J J. A simulation and mechanism analysis of long-term variations at land surface over arid/semi-arid area in north China. *J Geophys Res*, 2006, 111(D9): D09306
- 14 Huang M, Ji J, Li K. et al. The ecosystem carbon accumulation after conversion of grasslands to pine plantations in subtropical red soil of South China. *Tellus Ser B-Chem Phys Meteorol*, 2007, 59: 439—448
- 15 Ji J, Hu Y. A simple landsurface process model for use in climate study. *Acta Meteorol Sin (in Chinese)*, 1989, 3: 344—353
- 16 Yan Z, Ji J. A simple vegetation-soil-snowfall preliminary modeling. *Plateau Meteorol (in Chinese)*, 1995, 14(4): 415—424
- 17 Farquhar G D, Caemmerer S, Berry J A. A biochemical model of photosynthetic CO<sub>2</sub> assimilation in leaves of C<sub>3</sub> plants. *Planta*, 1980, 149: 78—90
- 18 Parton W J, Schimel D S, Cole C V, et al. Division S-3-soil microbiology and biochemistry: Analysis of factors controlling soil organic matter levels in great plains grasslands. *Soil Sci Soc Am J*, 1987, 51: 1173—1179
- 19 Cao M, Woodward F I. Net primary and ecosystem production and carbon stocks of terrestrial ecosystems and their responses to climate change. *Glob Change Biol*, 1998, 4: 185—198
- 20 Zhang S H, Peng G B, Huang M. The feature extraction and data fusion of regional soil textures based on GIS techniques. *Clim Environ Res (in Chinese)*, 2004, 9(1): 65—79
- 21 Box E O. Plant functional types and climate at the global scale. *J Veg Sci*, 1996, 7: 309—320
- 22 Xu Y L, Zhang Y, Lin Y H, et al. Validating PRECIS analyses on

- scenario of SRES B2 over China. *Chin Sci Bull*, 2006, 51(16): 2068–2072
- 23 Xu Y, Richard J. Validating PRECIS with ECMWF reanalysis data over China. *Chin J Agrometeorol* (in Chinese), 2004, 25(1): 5–9
- 24 Xu Y, Huang X, Zhang Y, et al. Statistical analyses of climate change scenarios over China in the 21st century. *Adv Clim Change Res* (in Chinese), 2005, 1(2): 80–83
- 25 Jones R G, Noguier M, Hassell D C, et al. *Generating High Resolution Climate Change Scenarios Using PRECIS*. Exeter: Met Office Hadley Centre, 2004. 1–35
- 26 Nakicenovic N, Alcamo J, Davis G, et al. *Special Report of Working Group III of the Intergovernmental Panel for Climate Change*. Cambridge: Cambridge University Press, 2000. 1–599
- 27 Li Y P, Ji J J. Simulations of carbon exchange between global terrestrial ecosystem and the atmosphere. *Acta Geogr Sin* (in Chinese), 2001, 56(4): 379–389
- 28 Dan L, Ji J J, He Y. Use of ISLSCP II data to intercompare and validate the terrestrial net primary production in a land surface model coupled to a general circulation model. *J Geophys Res*, 2007, 112: 1–18
- 29 Huang M, Ji J J, Cao M K, et al. Modeling study of vegetation shoot and root biomass in China. *Acta Ecol Sin* (in Chinese), 2006, 26(12): 4156–4163
- 30 Li K R, Wang S Q, Cao M K. Vegetation and Soil carbon storage in China. *Sci China Ser D-Earth Sci*, 2004, 47(1): 49–57
- 31 Li Z P, Han F X, Su Y, et al. Assessment of soil organic and carbonate carbon storage in China. *Geoderma*, 2007, 138: 119–126
- 32 Xie X L, Sun B, Zhou H Z, et al. Organic carbon density and storage in soils of China and spatial analysis. *Acta Pedol Sin* (in Chinese), 2004, 41(1): 35–43
- 33 Wang S Q, Zhou C H, Li K R. Analysis of soil organic carbon pool and the geographical distribution. *Acta Geogr*, 2000, 55(5): 533–544
- 34 Yu D S, Shi X Z, Wang H J, et al. Regional patterns of soil organic carbon stocks in China. *J Environ Manag*, 2007, 85(3): 680–689
- 35 Wu H, Guo Z, Peng C. Land use induced changes of organic carbon storage in soils of China. *Glob Change Biol*, 2003, 9: 305–315
- 36 Tao B, Li K R, Shao X M, et al. Temporal and spatial pattern of net primary production of terrestrial ecosystems in China. *Acta Geogr Sin* (in Chinese), 2003, 58(3): 372–380
- 37 Sun R, Zhu Q. Primary study on the effect of climate change on net primary productivity of terrestrial vegetation in China. *J Remote Sens*, 2001, 5(1): 58–61
- 38 Piao S, Fang J, Guo Q. Terrestrial net primary productivity and its spatio-temporal patterns in China during 1982–1999. *Acta Sci Nat Univ Peking* (in Chinese), 2001, 37 (4): 563–569
- 39 Xiao X M. Net primary production of terrestrial ecosystems in China and it's equilibrium responses to changes in climate and atmospheric CO<sub>2</sub> concentration. *Acta Phytoecol Sin* (in Chinese), 1998, 22(2): 97–118
- 40 Cao M K, Prince S D, Li K, et al. Response of terrestrial carbon uptake to climate interannual variability in China. *Glob Change Biol*, 2003(9): 536–546
- 41 He Y, Dong W, Ji J, et al. The net primary production simulation of terrestrial ecosystems in China by AVIM. *Adv Earth Sci* (in Chinese), 2005, 20(3): 345–349
- 42 Beerling D J, Woodward F I. *Vegetation and the Terrestrial Carbon Cycle: Modeling the First 400 Million Years*. Cambridge: Cambridge University Press, 2001
- 43 Ito A. Climate-related uncertainties in projections of the twenty-first century terrestrial carbon budget: Off-line model experiments using IPCC greenhouse-gas scenarios and AOGCM climate projections. *Clim Dyn*, 2005, 24: 435–448
- 44 Jenkinson D S, Adams D E, Wild A. Model estimates of CO<sub>2</sub> emissions from soil in response to global warming. *Nature*, 1991, 351: 304–306
- 45 Schimel D S, Braswell B H, Holland E A, et al. Climatic, edaphic and biotic controls over storage and turnover of carbon in soils. *Glob Biogeochem Cycles*, 1994, 8: 279–293
- 46 Kirschbaum M U F. The temperature dependence of soil organic matter decomposition and the effect of global warming on soil organic carbon storage. *Soil Biol Biochem*, 1995, 27: 753–760
- 47 Levy P E, Cannell M G R, Friend A D. Modelling the impact of future changes in climate, CO<sub>2</sub> concentration and land use on natural ecosystems and the terrestrial carbon sink. *Glob Environ Change*, 2004, 14: 21–31
- 48 Cramer W, Kicklighter D W, Bondeau A, et al. Comparing global modes of terrestrial net primary productivity(NPP): Overview and key results. *Glob Change Biol*, 1999, 5(Suppl): 1–15